Koopmans-compliant calculations on Hooke's atom

Semester project by Yannick Schubert, supervised by Dr. Edward Linscott and Dr. Andreas Adelmann
(Dated: January 26, 2022)

In this project, we examine the ability of Koopmans-compliant functionals to compute the electronic structure of Hooke's atom. We show that for this system they clearly outperform the widely used PBE functional in resembling the true exchange-correlation potential and in predicting quasiparticle energies.

I. INTRODUCTION

A. Koopmans Compliant Functionals

The possibility to obtain accurate first-principle predictions for quasi-particle related properties such as band gaps and photoemssion spectra is of central interest. Enhancing the design and characterization of optical and electronic devices such as solar cells is a possible application [1].

The recently developed Koopmans Compliant (KC) functionals [2–11] are one approach to calculate these spectral properties numerically. To test the performance of new developed functionals, it is essential to test them on systems with analytical solutions and on systems with accurate numerical and/or experimental reference solutions. Earlier studies have already shown that KC functionals work well for real molecules and solids when compared to the solutions obtained from accurate quantum chemistry methods, and to experimental results [12]. However, they have never been tested on an analytically solvable system. With an exact solution at hand the performance of different functionals can be evaluated in great detail. Hooke's atom is such a system. It describes two electrons confined in a harmonic potential.

In the following section a very short introduction to Kohn-Sham Density Functional Theory (KS-DFT) [13, 14] summarizes the basics needed to discuss some of its problems. Afterwards it will be motivated how KC functionals address these issues.

1. Summary of standard Kohn-Sham-DFT

The overall goal of all functionals discussed in this study is to computationally model a system of interacting electrons in a given external potential $\hat{V}_{ext}$. Even without the spin degrees of freedom, the corresponding Schrödinger equation is a differential equation in $3N$ dimensional space. Solving this equation directly for practically every system of interest vastly exceeds today's (and tomorrow's) computational capabilities, so we must necessarily make some approximations.

There are several different approaches one can take here. High-level perturbative methods like Green's-function-based approaches [15] (e.g. the GW approximation [16]) and wavefunction-based approaches (e.g. coupled cluster [17] or Quantum Monte Carlo [18]) are accurate but computationally expensive, which limits what systems we can study with these approaches.

A more approximate and computationally inexpensive approach is density functional theory (DFT). DFT introduces a framework that allows us to reformulate the complicated many-body particle problem as a set of N independent single-particle problems and therefore tremendously reduces the complexity. Its main ideas are based on the theorems by Hohenberg and Kohn [13]. They imply that all properties of the system of interacting electrons are completely determined by the ground state density and that the total energy as a functional of the density alone suffices to calculate the exact ground state energy and ground state density. From this it can be inferred that all physical quantities can as well be considered as functionals of the density instead of as functionals of the many-body wavefunction. However, this is only a statement about the existence of such functionals and not about how they can be found.

A central observation of Kohn and Sham [14] provides remedy. They discovered that finding the ground-state energy and density of our system of interacting electrons is equivalent to finding the ground-state energy and density of an auxiliary system of non-interacting electrons. Any state in such a system of non-interacting electrons can be expressed as a single Slater determinant over single-particle wavefunctions ϕ_j^{KS}, where the index j summarizes all necessary quantum numbers. For the system of non-interacting electrons, a set of N single-particle equations, called Kohn-Sham equations, can be derived:

$$\text{KS 1: } \left[-\frac{1}{2}\nabla^2 + v_{\mathrm{eff}}[\rho](\mathbf{r})\right]\phi_j^{\mathrm{KS}}(\mathbf{r}) = \varepsilon_j^{\mathrm{KS}}\phi_j^{\mathrm{KS}}(\mathbf{r})$$

$$\text{KS 2: } v_{\mathrm{eff}}[\rho](\mathbf{r}) = v_{\mathrm{H}}[\rho](\mathbf{r}) + v_{\mathrm{ext}}(\mathbf{r}) + v_{\mathrm{xc}}[\rho](\mathbf{r})$$

$$v_{\mathrm{H}}[\rho](\mathbf{r}) = \int d^3\mathbf{r}\frac{\rho(\mathbf{r}')}{|\mathbf{r}-\mathbf{r}'|}$$

$$\rho(\mathbf{r}) = \sum_j^{\mathrm{occ}} |\phi_j^{\mathrm{KS}}(\mathbf{r})|^2$$

Here, v_{H} is the Hartree potential, v_{ext} is the external potential and $-\frac{1}{2}\nabla^2$ is the kinetic energy operator. The exchange-correlation potential v_{xc} is constructed in such a way that it contains all unknown terms and that its contribution to the total energy is small compared to the contributions of the Hartree potential, of the external potential and of the kinetic energy operator. The $\varepsilon_j^{\mathrm{KS}}$ are the so-called Kohn-Sham eigenvalues and ρ(r) is the

electronic ground-state density. By construction of the Kohn-Sham equation this density is equal to the exact ground-state density of the interacting system.

These equations have to be solved self-consistently, since the effective potential v_{eff} is a functional of the density, which in turn is constructed out of the single-particle wavefunctions $\{\phi_j\}$ that solve the first equation.

If the exchange-correlation potential was known, the Kohn-Sham equations would be an exact reformulation of the original many-body problem without any approximations being made. Unfortunately, it is unknown in nearly all cases of interest. To nevertheless benefit from the reduced complexity of the single-particle framework, the exchange and the correlation potential can be approximated in various ways. Two famous classes of approximations are the so-called local density approximation (LDA) and generalized gradient approximations (GGA). LDA is the simplest approximation of the exchange-correlation potential. Is assumes that it is a functional of the local density only. The GGA describe the next level of approximation, where we assume that the exchange-correlation functional is not only a functional of the density but also of the gradient of the density. Such a functional is called semi-local. A very common example of the functionals belonging to the class of GGA functionals is the so-called PBE functional [19].

2. *Problems of Kohn-Sham DFT*

A common approach in physics and chemistry to describe a complicated many-body quantum state is to only focus on the low-energy excitations and treating them as weakly interacting quasi-particles. In our case we are primarily interested in electronic excitations and therefore electronic quasi-particles (hereafter just referred to as quasi-particles). These move in an effective field generated by all other electrons and the nuclei. The quasi-particle energy describes the energy that is needed to remove it from the system. Accordingly, the difference between two quasi-particle energies is the energy needed to excite the system from one state to another. Therefore, if we can accurately predict quasi-particle energies, we can predict properties such as conductivity and optical absorption.

One of the fundamental problems with KS-DFT is that the KS orbital energies $\{\varepsilon_j^{KS}\}$ are theoretically unrelated to those quasi-particle energies. As shown in the previous subsection, they are only the single-particle energies of some auxiliary system that happens to have the same ground state density as the system of interest. Nevertheless, in practice the KS eigenenergies often qualitatively (and sometimes even quantitiatively) compare well to experiment, and it is standard practice to treat KS eigenenergies as quasi-particle energies

But even if the first problem was ignored, errors introduced when approximating the exchange-correlation potential imply that the Kohn-Sham energies are bad approximations for quasi-particle energies.

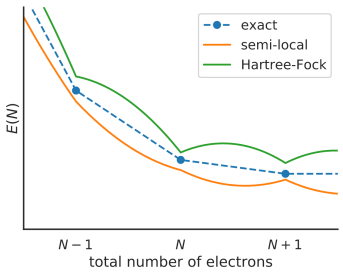

FIG. 1. $E(N)$ for the exact exchange-correlation functional, semi-local DFT and Hartree Fock

One typical error is the so-called self-interaction error (SIE). It accounts for the error that exists when the non-physical self-interaction which is part of the Hartree potential is not perfectly canceled by the exchange-correlation potential. For a single Slater determinant, the exact Hartee potential $v_{\text{H},i}$ felt by the particle i is given by

$$v_{\text{H,i}}(\mathbf{r}) = \sum_{j \neq i} \int d\mathbf{r}' \frac{|\phi_j(\mathbf{r}')|^2}{|\mathbf{r} - \mathbf{r}'|}$$

As shown above, in KS-DFT the Hartree potential is

$$v_{\text{H}}(\mathbf{r}) = \int d\mathbf{r}' \frac{\rho(\mathbf{r}')}{|\mathbf{r} - \mathbf{r}'|} = \sum_j \int d\mathbf{r}' \frac{|\phi_j^{\text{KS}}(\mathbf{r}')|^2}{|\mathbf{r} - \mathbf{r}'|}$$

where in contrast to $v_{\text{H},i}$ the sum also contains the term $j = i$. The KS equations are still exact since the exact exchange-correlation potential perfectly compensates this difference. But in practice, most approximations of it do not. This is called the "one-body self interaction error". As a consequence the electrons of the KS solution are over-delocalized. That means that their wavefunctions are artificially spread out, in order to minimize the Coulomb repulsion they feel from their own density.

It has recently been argued that the concept of the one-electron self-interaction error can be generalized to the "many-body self-interaction error", which manifests itself as a curvature in the total energy as a function of the total number of electrons [20] as schematically shown in fig. 1. However, the exact functional is piecewise linear with respect to the total number of electrons [21].

Janak showed [22] that if we have the exact exchange-correlation potential, the Kohn-Sham orbital energy is given by the derivative of the total energy with respect to the occupation of the corresponding state:

$$\varepsilon_j^{\text{KS}} = \frac{dE}{df_j}$$

From this it follows that the wrong curvature directly affects KS eigenvalues which we would like to interpret as quasi-particle energies.

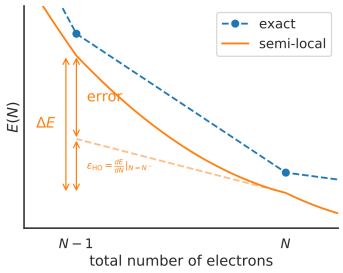

FIG. 2. Consequence of the SIE of semi-local DFT for quasi-particle energies

3. *How do KC functionals address the problems of KS-DFT?*

To overcome some of the KS-DFT issues a piecewise linearity (PWL) constraint to the total energy as a function of the particle number can be introduced. Thanks to Janak's theorem, this is equivalent to saying that the orbital energy of the highest occupied state should be a constant as a function of its occupation. We call this state the HOMO (highest occupied molecular orbital).

Koopmans spectral functionals are a class of corrective functionals that bridge the gap between KS eigenvalues and quasi-particle energies and remedy the SIE. In order to achieve this, these functionals generalize the idea of PWL in the sense that they enforce a constant orbital energy for any orbital in the system, rather than only for the highest-energy state.

Denote with $\tilde{\varepsilon}_i$ the energy of the quasi-particle i. Assuming PWL and making use of Janak's theorem $\tilde{\varepsilon}_i$ can be calculated to be equal to the corresponding Kohn-Sham orbital energy:

$$\begin{aligned}\tilde{\varepsilon}_i \equiv E(N) - E_i(N-1) &= \frac{E(N) - E_i(N-1)}{N - (N-1)} \\ &\overset{PWL}{=} \frac{\partial E}{\partial f_i} \overset{Janak}{=} \varepsilon_i^{\mathrm{KS}}\end{aligned} \tag{1}$$

where $E_i(N-1)$ is the total energy of the system where we have removed the quasi-particle i from the system. Therefore, the PWL would cure the first problem, allowing the KS energies to be interpreted as quasi-particle energies.

Moreover, the generalized PWL condition guarantees that the orbital energies do not depend on the occupation of the orbital itself. Therefore the orbital's energy is free from the self-interaction error.

4. *Linearization in KC functionals*

The KC functionals are constructed (following Ref. 9) as corrective functionals: that is, they start from a DFT energy functional E^{DFT} (the "base" functional) and add a correction Π_j to each orbital j such that the total energy E^{KC} is linear with respect to the fractional occupation f_j.

To motivate how this could be achieved, consider frozen orbitals first, i.e. neglect the response of all electrons as the occupation of one orbital is changed. In this case a KC correction Π_j^{KC} for each orbital j should linearize the total energy:

$$\begin{aligned}&\text{Ansatz: } E^{\mathrm{KC}} = E^{\mathrm{DFT}} + \sum_j \Pi_j^{\mathrm{KC}} \\ &\Rightarrow \eta_i \equiv \text{const} \overset{!}{=} \frac{\partial E^{\mathrm{KC}}}{\partial f_i} = \frac{\partial E^{\mathrm{DFT}}}{\partial f_i} + \frac{\partial \Pi_i^{\mathrm{KC}}}{\partial f_i} \\ &\Rightarrow \eta_i - \frac{\partial \Pi_i^{\mathrm{KC}}}{\partial f_i} = \frac{\partial E^{\mathrm{DFT}}}{\partial f_i} \overset{\text{Janak}}{=} \varepsilon_i^{\mathrm{KS}} = \langle \varphi_i | \hat{H}^{\mathrm{DFT}}(f_i) | \varphi_i \rangle \\ &\Rightarrow \Pi_i^{\mathrm{KC}} = -\int_0^{f_i} ds \langle \varphi_i | \hat{H}^{\mathrm{DFT}}(s) | \varphi_i \rangle + f_i \eta_i\end{aligned}$$

$\hat{H}^{\mathrm{DFT}}(s)$ is the KS Hamiltonian of the base functional calculated with a fractional occupation s in the orbital φ_i. The constant η_i can be chosen in different ways, the so-called KI and KIPZ methods denote two of them. Note that in contrast to standard KS-DFT energy functionals the KC energy functional is not only dependent on the total density but also on the occupations of each orbital f_i. In case of such orbital-density dependent (ODD) corrections we have to minimize the total energy functional with respect to the entire set of orbitals and not just with respect to the total density. The set of orbitals that minimize the total energy is called the variational orbitals. In this orbital dependent DFT (ODDFT) framework these are in general not the same as the so-called canonical orbitals, which are the states that diagonalize the Hamiltonian.

A conjugate gradient algorithm is employed to variationally minimize the energy functional with respect to the variational orbitals.

To account for the relaxation of the other electrons, orbital-dependent screening parameters α_i are introduced. In total, the KC energy functional reads:

$$E^{\mathrm{KC}}[\rho, \{f_i\}, \{\alpha_i\}] = E^{\mathrm{DFT}}[\rho] + \sum_j \alpha_j \Pi_j^{\mathrm{KC}}[\rho, \{f_i\}] \tag{2}$$

The screening parameters are defined such that $\varepsilon_i^{KC} = \Delta E_i^{KC}$ holds for relaxed orbitals instead of frozen orbitals, where

$$\Delta E_i^{\mathrm{KC}} = \begin{cases} E^{\mathrm{KC}}(N) - E_i^{\mathrm{KC}}(N-1) & \text{filled orbitals} \\ E_i^{\mathrm{KC}}(N+1) - E^{\mathrm{KC}}(N) & \text{empty orbitals} \end{cases}$$

This definition of the screening parameters can be employed to compute them ab inito. The method that is used in this project is the so-called ΔSCF approach. It is an iterative procedure relying on a series of Koopmans and DFT calculations.

This method takes its name from the well established ΔSCF scheme [23] for standard KS-DFT functionals,

where total energy differences are used to get more accurate estimations of quasi-particle energies. For example we can conduct two DFT calculations, one with N electrons and one with $N-1$ electrons. The difference in total energy gives an estimate for the HOMO energy:

$$\varepsilon_{\mathrm{HOMO}}^{\mathrm{DFT,\Delta SCF}} = E^{\mathrm{DFT}}(N) - E^{\mathrm{DFT}}(N-1) \tag{3}$$

While the HOMO energies obtained from a single LDA or GGA calculation are very prone to the SIE, this method only relies on total energies calculated at integer occupations. Since total energies are ground state properties they can be accurately predicted by DFT according to the theorems of Hohenberg and Kohn. Therefore, the ΔSCF method yields much more accurate HOMO energies than single LDA or GGA calculations.

By construction of the screening parameters, the HOMO energy of the KI method will converge to the HOMO energy of the underlying "base" functional if in both cases the ΔSCF method is used. The reason for this is that for integer occupations the total KI energy (and therefore also its ground state density) is equal to the total energy obtained with the underlying DFT method. This is not the case for the KIPZ method, which also modifies the density.

B. Hooke's Atom

Now that we have introduced the functionals which we want to study, we can introduce the system that we will use to asses their performances. It is called Hooke's atom and it is describing a system where two electrons are exposed to an external harmonic potential. The Hamiltonian describing this system is given by:

$$\mathcal{H} = -\frac{1}{2}\left(\nabla_1^2 + \nabla_2^2\right) + \frac{1}{2}k\left(r_1^2 + r_2^2\right) + \frac{1}{r_{12}}$$

For $k = \frac{1}{4}$ the Schrödinger equation can be solved analytically [24] and the exact ground state wavefunction can be expressed as:

$$\Psi(\mathbf{r}_1, \mathbf{r}_2) = N_0 \times \left(1 + \frac{1}{2}\left|\mathbf{r}_1 - \mathbf{r}_2\right|\right) e^{-\frac{1}{4}\left(r_1^2 + r_2^2\right)}$$

It has an energy of

$$E = 2 \text{ Hartree} \tag{4}$$

N_0 denotes the normalization constant.

The ground state density is given by:

$$\begin{aligned}\rho(\mathbf{r}) &= 2\int d\mathbf{r}_2 \left|\Psi(\mathbf{r}, \mathbf{r}_2)\right|^2 \\ &= 2N_0^2 e^{-1/2r^2}\left\{\left(\frac{\pi}{2}\right)^{1/2}\left[\frac{7}{4} + \frac{1}{4}r^2 \right.\right. \\ &\qquad \left.\left. + \left(r + \frac{1}{r}\right)\operatorname{erf}\left(2^{-1/2}r\right)\right] + e^{-1/2r^2}\right\}\end{aligned} \tag{5}$$

We can also extract various quantities as predicted by the exact DFT functional. For example, the density given by the exact DFT functional will match exactly the analytical solution. Furthermore, we can obtain analytical solutions for the exchange-correlation potential and the KS energy eigenvalues (see appendix A 1 for details). Moreover it can be shown how to express the KC correction to the exchange-correlation potential and to the HOMO energy as a functional of quantities obtained by the "base" functional (see appendix A 2 for details).

II. COMPUTATIONAL METHODS

We simulated Hooke's atom within Quantum Espresso [25, 26] (QE). The harmonic potential was achieved by constructing a "hookium" pseudopotential with the correct r^2 behaviour at small distances (see appendix B 1 for details). We used an energy cutoff of 50 Ry, a cell size of 12.5 Å, and a cutoff of the potential of 5.0 Å. We chose those parameters as the result of a convergence analysis (see appendix B 2 for details). We performed the calculations with the LDA, PBE, PZ, KI, and KIPZ functionals. For the KI and KIPZ calculations we used PBE as a "base" functional. The PZ ("Perdew-Zunger Self-Interaction-Corrected") functional is the PBE functional with the v_{Hxc}-potential removed orbital-by-orbital [27].

III. RESULTS

In the following we will present the densities, the exchange-correlation potentials and the exchange-correlation energies obtained for the different functionals.

The converged densities as well as the exact density as given by eq. (5) are depicted in fig. 3. The KI density is exactly equal to the PBE density. This is also expected as discussed in section I A 4. By contrast, the KIPZ calculation does modify the density. While for small distances the LDA and PBE densities are too small compared to the exact density, the PZ and the KIPZ densities are too large. On the one hand, the LDA and PBE orbitals are over-delocalized due to the SIE. On the other hand, KIPZ and PZ are both methods that explicitly target to correct the one-body SIE but seem to overshoot for this two-electron system.

Figure 4 shows the approximation of the exchange-correlation potential of the different functionals in comparison to the exact exchange-correlation functional as derived in eq. (A2). The ODD correction for the KI, KIPZ and PZ case correspond to the formulas given in eq. (A7), eq. (A8) and eq. (A9) respectively. As expected, the v^{KI} potential correction implies just a constant shift to PBE exchange-correlation potential. Therefore it fails in the same way as PBE to reproduce the asymptotic Coulombic decay of the exact potential. The KIPZ po-

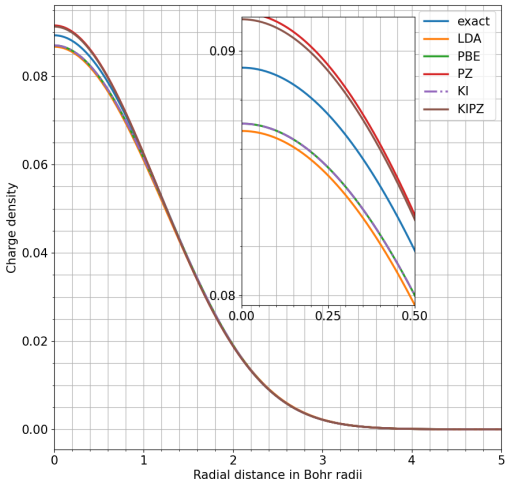

FIG. 3. Electron Density of the different approximations compared to the exact electron density. The electron density is in all cases normalized such that integrating $4\pi r^2 \rho(r)$ from zero to infinity gives two. All quantities are plotted along a one-dimensional line starting from the origin of the potential.

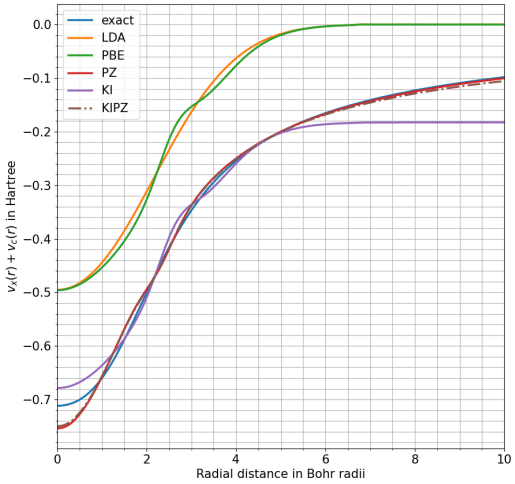

FIG. 4. For the DFT functionals we plot the xc potential. For the ODDFT functionals we plot the xc potential of the base functional, plus the orbital-specific correction. All quantities are plotted along a one-dimensional line starting from the origin of the potential.

tential corrects this, and gives a much closer agreement for large distances. The PZ methods gives a similar result which can be motivated from the discussion in appendix A 2.

In fig. 5 the functionals are applied to the respective KS orbitals which can be calculated from the density

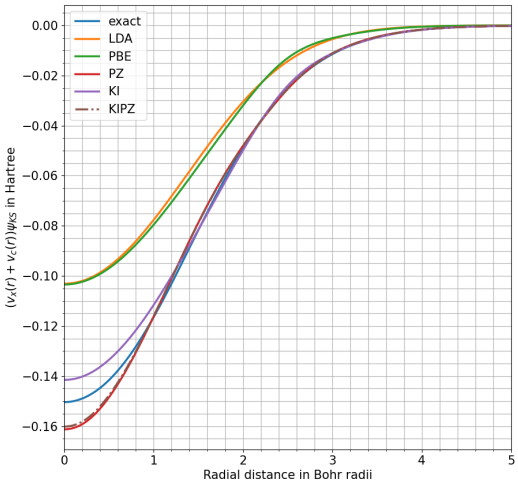

FIG. 5. We apply the potential plotted in fig. 5 to the single-electron wavefunction. All quantities are plotted along a one-dimensional line starting from the origin of the potential.

TABLE I. The total energies and HOMO energies obtained with different functionals in Hartree. In parentheses the difference to the exact HOMO energy is given in per cent.

Functional	Total Energy	HOMO Energy
Exact	2.0000	1.2500
LDA	2.0257	1.4446 (+15.57%)
PBE	2.0090	1.4391 (+15.13%)
ΔSCF		1.2564 (+ 0.51%)
PZ	2.0059	1.2563 (+ 0.50%)
KI	2.0090	1.2564 (+ 0.52%)
KIPZ	2.0061	1.2560 (+ 0.48%)

as $\phi(\mathbf{r}) = [\frac{1}{2}\rho(\mathbf{r})]^{1/2}$ as motivated in eq. (A1). This is a key physical quantity since during the minimization procedure of the total energy we only ever consider the potential multiplied with the wavefunction and never just the potential.

The results for the total energies are shown in table I. Since this is a ground state property, all functionals obtain total energies that are very close to the one given in eq. (4). The results also reflect the fact that the Koopmans functionals are not primarily made to get better approximations of the total energy but to predict orbital energies more accurately.

Finally, we consider the HOMO energies that we obtain with the different functionals and compare them to the exact solution given in eq. (A3). The results are shown in table I. The HOMO energy of the PBE calculation is approximately 0.189 Hartree higher than the exact HOMO energy. A much closer result with PBE is achieved using the ΔSCF method. It yields a result that is just 0.0064 Hartree higher than the exact value. As

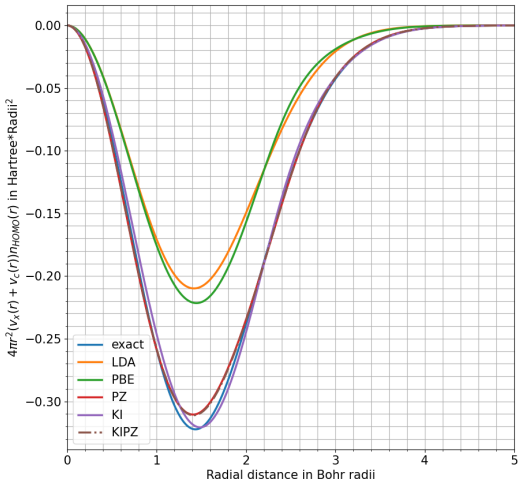

FIG. 6. We multiply the potential plotted in fig. 5 with $4\pi r^2 n_{HOMO}(r)$. All quantities are plotted along a one-dimensional line starting from the origin of the potential.

elaborated in section I A 4 this gives the same result as the KI method. The KIPZ and the PZ methods give an additional slight improvement compared to the KI result.

To get the contribution of the exchange correlation potential to the HOMO energy we have to multiply the potential shown in fig. 4 with the orbtial density and $4\pi r^2$ and integrate it over all radial distances. To visualize this integrand, the total exchange-correlation potential (including ODD corrections for the ODDFT methods) multiplied with $4\pi r^2 n_{\mathrm{HOMO}}$ is shown in fig. 6. As we can conclude from this figure neither very small distances nor very large distances contribute much to the integral.

IV. CONCLUSION

Koopmans functionals do an excellent job of reproducing the total energy, the HOMO energy, and the exact KS potential for Hooke's atom.

The PBE and LDA orbitals are over-delocalized due to self-interaction error. This is reflected by a too small density at small distances. KIPZ seems to over-decompensate this effect, since the electrons are too localized.

As for most real materials a single PBE calculation also fails for this simple system to produce an accurate result for the HOMO energy. The ΔSCF method does a much better job since it only relies on total energy calculations.

Compared to the KI potential the main improvement when using the KIPZ method in approximating the exact exchange-correlation potential is achieved for large distances. Since the electron density vanishes for large distances, the effect on the HOMO energy is small. Therefore the KIPZ method only yields a small improvement in approximating the HOMO energy compared to the KI result in the case of Hooke's atom. As motivated in appendix A 2, in our simple system the PZ correction yields similar results as the KIPZ correction.

As a final note we would like to mention that this study has some limitations mainly due to the simplicity of Hooke's atom. For example, it does not allow investigating the implications of having two sets of orbitals, canonical and variational. The reason for that is that for such a one-orbtial system the Hamiltonian is not a matrix but a number and therefore the canonical orbitals are identical to the variational orbitals.

As an outlook we would like to include an empty state in the calculation which would enable us to compute the LUMO energy (lowest unoccupied molecular orbital). This quantity would allow us to predict the minimal excitation energy, which is given by the difference between the LUMO and the HOMO energy. For this calculation we would expect that the KI and KIPZ methods perform better than the PZ method, since the PZ method exclusively adds a correction to filled states.

Appendix A: Eigenvalues and Exchange-Correlation Functionals for Hooke's Atom

1. Kohn-Sham Functionals

In the following it will be shown how exact expressions for the exchange and correlation potentials and for the HOMO energy can be obtained for Hooke's atom [28].

For two electrons of opposite spin, the two KS single-orbital wave functions $\phi_i^{\mathrm{KS}} \equiv \phi^{\mathrm{KS}}$ and energies $\varepsilon_i^{\mathrm{KS}} \equiv \varepsilon^{\mathrm{KS}}$ are identical. As described in section I A 1 the exact ground state electron density of the system is the same as the density of the non-interacting Kohn-Sham system. From this, the exact KS orbital wave functions ϕ^{KS} can be calculated:

$$\rho(\mathbf{r}) = 2\left|\phi^{\mathrm{KS}}(\mathbf{r})\right|^2 \Rightarrow \phi^{\mathrm{KS}}(\mathbf{r}) = \left[\frac{1}{2}\rho(\mathbf{r})\right]^{1/2} \tag{A1}$$

This can be employed to invert the Kohn-Sham equations and to obtain an expression for the exchange-correlation potential:

$$v_{\mathrm{xc}}[\rho](\mathbf{r}) = \varepsilon^{\mathrm{KS}} - v_{\mathrm{ext}}(\mathbf{r}) - v_{\mathrm{H}}[\rho](\mathbf{r}) - v_{\mathrm{KE}}[\rho] \tag{A2}$$

where the last term comes from the kinetic energy

$$v_{\mathrm{KE}}[\rho] = -\frac{1}{2}\frac{\nabla^2\phi}{\phi} = \frac{1}{4}\left(\frac{\nabla^2\rho}{\rho}\right) - \frac{1}{8}\left(\frac{\nabla\rho}{\rho}\right)^2$$

The external potential v_{ext} in this case is given by $v_{\mathrm{ext}}(\mathbf{r}) = \frac{1}{2}kr^2$ and v_{H} is the Hartree potential $v_{\mathrm{H}} = \int d^3\mathbf{r}\frac{\rho(\mathbf{r}')}{|\mathbf{r}-\mathbf{r}'|}$ as before. The orbital energy $\varepsilon_{\mathrm{KS}}$ can be calculated as follows:

$$\varepsilon^{\mathrm{KS}} \equiv \varepsilon^{\mathrm{KS}}_{\mathrm{HOMO}} = E(N) - E(N-1)$$

$E(2) = 2$ Hartree is the ground state energy of Hooke's atom and $E(1) = \frac{3}{2}k^{1/2} = \frac{3}{4}$ Hartree is the energy of a single electron in a three dimensional harmonic potential. This implies

$$\varepsilon^{\mathrm{KS}} = \frac{5}{4}\ \text{Hartree} \tag{A3}$$

Therefore all terms on the right of eq. (A2) are known exactly and v_{xc} can be inferred.

For two electrons of opposite spin, the exchange potential is just half of minus the Hartree potential

$$v_{\mathrm{x}}[\rho](\mathbf{r}) = -\frac{1}{2}v_{\mathrm{H}}[\rho](\mathbf{r}) \tag{A4}$$

The exact correlation potential is then given by

$$v_{\mathrm{c}}[\rho](\mathbf{r}) = v_{\mathrm{xc}}[\rho](\mathbf{r}) - v_{\mathrm{x}}[\rho](\mathbf{r}) \tag{A5}$$

2. Orbital Density Dependent corrections

The KC corrections as well as the PZ correction introduce orbital density dependent (ODD) corrections to the total energy. That means that the energy is no longer only a functional of the total density but also of the orbital density $\rho_i = f_i n_i(\mathbf{r})$, where $n_i(\mathbf{r}) = |\phi_i(\mathbf{r})|^2$ is the occupation-independent density and f_i is the occupation of the orbtial i.

From these corrections to the total energy, an ODD correction to the exchange-correlation potential can be defined by taking the functional derivative with respect to the density. In the case of the KC-potential it is given by:

$$\hat{v_i}^{\mathrm{KC}} = \frac{\delta}{\delta\rho_i}\sum_j \Pi_j^{\mathrm{KC}} \tag{A6}$$

The general form of this potential for the KI and the KIPZ cases is presented in [5]. In our two electron system there is only one orbital and therefore the spin quantum number σ is sufficient to describe the state i. Since each spin-channel σ is fully occupied, i.e. $n_\sigma = \rho_\sigma = \frac{1}{2}\rho$, the general expression can be simplified to

$$\begin{aligned}\hat{v}_\sigma^{\mathrm{KI}}(\mathbf{r})|_{f_\sigma=1} &= -E_{\mathrm{Hxc}}\left[\frac{1}{2}\rho\right] + E_{\mathrm{Hxc}}\left[\rho\right] \\ &\quad - \frac{1}{2}\int d\mathbf{r}' v_{\mathrm{Hxc}}\left[\rho\right](\mathbf{r}')\rho(\mathbf{r}') \end{aligned} \tag{A7}$$

$$\begin{aligned}\hat{v}_\sigma^{\mathrm{KIPZ}}(\mathbf{r})|_{f_\sigma=1} &= \hat{v}_\sigma^{\mathrm{KI}}(\mathbf{r})|_{f_\sigma=1} \\ &\quad - E_{\mathrm{Hxc}}\left[\frac{1}{2}\rho\right] - v_{\mathrm{Hxc}}\left[\frac{1}{2}\rho\right](\mathbf{r}) \\ &\quad + \frac{1}{2}\int d\mathbf{r}' v_{\mathrm{Hxc}}[\rho](\mathbf{r}')\rho(\mathbf{r}') \\ &= \left(E_{xc}\left[\rho\right] - 2E_{xc}\left[\frac{1}{2}\rho\right]\right) - v_{Hxc}\left[\frac{1}{2}\rho\right](\mathbf{r}) \end{aligned} \tag{A8}$$

The subscript Hxc indicates that we take the sum of Hartree, exchange and correlation contributions. Note that the KI potential does not depend on $\mathbf{r}$ in our case. Moreover, the potential will be the same for both electrons. Therefore, we can also drop the spin index σ. To include screening we multiply each expression above with the screening parameter α_i of the corresponding orbital i.

The PZ correction removes the v_{Hxc}-potential from each orbital, i.e. the PZ orbital dependent correction is in general given by

$$\hat{v}_i^{PZ}(\mathbf{r}) = -v_{Hxc}[\rho_i](\mathbf{r})$$

This expression can again be simplified in the case of Hooke's atom:

$$\hat{v}_\sigma^{\mathrm{PZ}}(\mathbf{r})|_{f_\sigma=1} = -v_{Hxc}\left[\frac{1}{2}\rho\right](\mathbf{r}) \tag{A9}$$

Janak's theorem eq. (1) can be used to derive how the ODD potentials affect the HOMO energy in the simple case of Hooke's atom:

$$\begin{aligned}\varepsilon_{\mathrm{HOMO}}^{\mathrm{KC}}[\rho] &= \varepsilon_{\mathrm{HOMO}}^{\mathrm{DFT}}[\rho] \\ &\quad + \alpha_{\mathrm{HOMO}}\int d\mathbf{r} v^{\mathrm{KC}}(\mathbf{r}) n_{\mathrm{HOMO}}(\mathbf{r}) \end{aligned} \tag{A10}$$

$$\begin{aligned}\varepsilon_{\mathrm{HOMO}}^{\mathrm{PZ}}[\rho] &= \varepsilon_{\mathrm{HOMO}}^{\mathrm{DFT}}[\rho] \\ &\quad + \int d\mathbf{r} v^{\mathrm{PZ}}(\mathbf{r}) n_{\mathrm{HOMO}}(\mathbf{r}) \end{aligned} \tag{A11}$$

If we neglected orbital relaxation, i.e. set the screening parameters to 1, in our case the PZ and the KIPZ potential would be identical except for a constant shift. Therefore they would yield the same density and hence the same total energy. Since the electrons in Hooke's atom screen only very little, both corrections yield similar densities, potentials and energies.

Appendix B: Compuational Methods

1. The Pseudopotential

In order to simulate Hooke's atom with DFT, we need to somehow create a background harmonic potential within the framework of QE. When simulating real molecules or solids, the background potential is the potential due to the nucleii and the core electrons, typically represented by an effective potential called a "pseudopotential". Pseudopotentials allow us to focus on the valence electrons for the actual computation and therefore reducing the complexity of the problem. The idea behind this is that the core electrons are very inert to the local environment.

However, we can't simply create a harmonic pseudopotential and deploy it in QE. This is because for asymptotic distances from the nucleus QE expects the pseudopotential to behave like the Coulomb potential of a

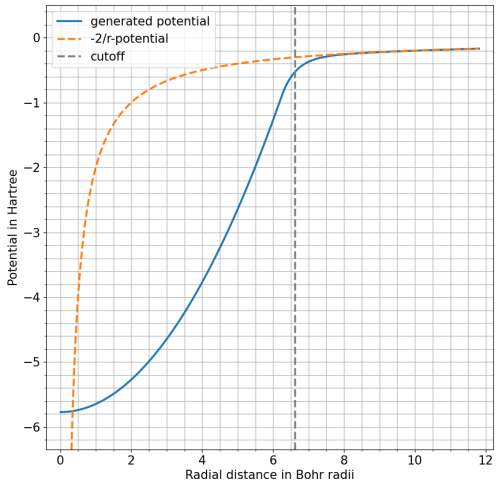

FIG. 7. Input potential with a cutoff of the potential of 3.5 Å (shown in blue). For large distances the potential behaves like the Coulombic potential of a Helium nucleus (shown in yellow).

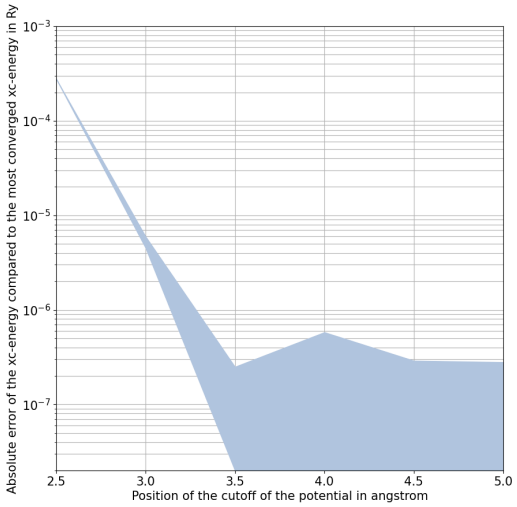

FIG. 8. Absolute deviation from the most converged result of the exchange-correlation energy obtained with PBE for different combinations of the parameters pot_cut, cellsize and ecutwfc. The latter two are summarized by the blue area.

point charge. That means, asymptotically it should be equal to $-Z_{\text{val}}/r$, where Z_{val} is the number of valence electrons and r is the distance from the nucleus.

The input potential that we created to solve Hooke's atom is a shifted harmonic potential for small distances and the expected Coulombic potential for large distances. We implemented an exponential decay between those two regimes to make the potential continuously differentiable. The position of the transition between the two regimes can be characterized by a parameter that we call r_c. Figure 7 shows the potential generated for r_c being equal to 3.5 Å.

2. Convergence Analysis

It is very important that the cutoff of the potential does not influence any physical quantities obtained by the simulation. Otherwise it would no longer be possible to compare the results to the exact solution, since the situation could no longer be described by two electrons in a harmonic potential. To ensure this, r_c has to be set to large enough radial distances.

Apart from a large enough r_c, it is essential, that the results are also converged with respect to the size of the simulated unit cell ("cellsize") and with respect to the kinetic energy cutoff ("ecutwfc"). To ensure this, we performed a convergence analysis with respect to these three parameters. More specifically, we computed the exchange-correlation energy with the PBE functional for the following ranges of the three parameters:

$$r_c \in \{2.5\ \text{Å}, 3.0\ \text{Å}, 3.5\ \text{Å}, 4.0\ \text{Å}, 4.5\ \text{Å}, 5.0\ \text{Å}\}$$
$$\text{cellsize} \in \{10.0\ \text{Å}, 11.25\ \text{Å}, 12.5\ \text{Å}, 13.75\ \text{Å}, 15.0\ \text{Å}\}$$
$$\text{ecutwfc} \in \{50\ \text{Ry}, 60\ \text{Ry}, 70\ \text{Ry}, 80\ \text{Ry}, 90\ \text{Ry}, 100\ \text{Ry}\}$$

We compare each result to the result that we obtain with $r_c = 5.0$ Å, cellsize $= 15.0$ Å and ecutwfc $= 100$ Ry. We assume this calculation to yield the most converged result.

It turned out that the position of the cutoff of the potential had the biggest impact on the deviation from the most converged result. In the chosen range of parameters it was impossible to identify any trend with respect to the kinetic energy cut-off and the size of the unit cell. As can be seen clearly in fig. 8 the result is well converged for a cutoff of the potential at 3.5 Å. Therefore we took this value as the cutoff of the potential for all calculations. As kinetic energy cutoff we used the smallest tested value of 50 Ry since higher values did not yield better results in the convergence analysis. And for the cell size we selected 12.5 Å to ensure that the exponential decay between the two regimes has converged to the Helium-like behavior well before the cell boundary to prevent any kind of unwanted discontinuities.

Appendix C: Exchange and Correlation Energies for LDA and PBE

For the PBE and the LDA functional it is possible to extract the exchange and the correlation potential individually. These potentals can be compared to the exact

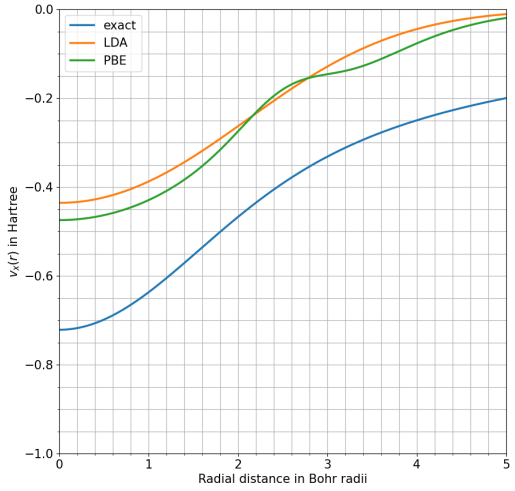

FIG. 9. Exchange potential of the LDA and PBE approximation computed with QE compared to the exact exchange potential. All quantities are plotted along a one-dimensional line starting from the origin of the potential.

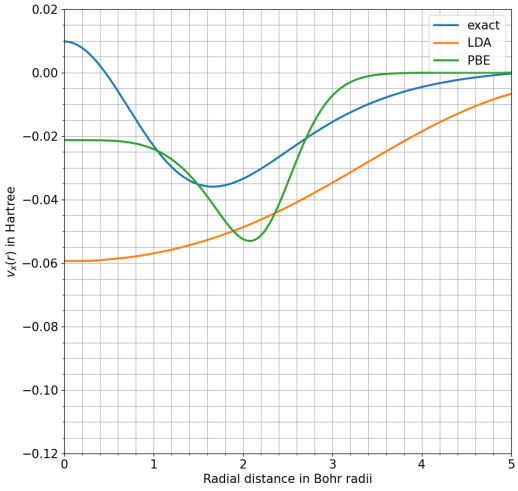

FIG. 10. Correlation potential of the LDA and PBE approximation computed with QE compared to the exact exchange potential. All quantities are plotted along a one-dimensional line starting from the origin of the potential.

expressions eq. (A4) and eq. (A5) as shown in fig. 9 and fig. 10. These plots reproduce exactly the results presented in [29].

[1] I. Dabo, A. Ferretti, C. H. Park, N. Poilvert, Y. Li, M. Cococcioni, and N. Marzari, Physical Chemistry Chemical Physics **15**, 685 (2013), arXiv: 1210.7973.

[2] I. Dabo, M. Cococcioni, and N. Marzari, Non-koopmans corrections in density-functional theory: Self-interaction revisited (2009), arXiv:0901.2637 [cond-mat.mtrl-sci].

[3] I. Dabo, A. Ferretti, N. Poilvert, Y. Li, N. Marzari, and M. Cococcioni, Physical Review B **82**, 115121 (2010), publisher: American Physical Society.

[4] I. Dabo, A. Ferretti, and N. Marzari, Topics in current chemistry **347**, 193 (2014).

[5] G. Borghi, A. Ferretti, N. L. Nguyen, I. Dabo, and N. Marzari, Physical Review B **90**, 075135 (2014), publisher: American Physical Society.

[6] G. Borghi, C. H. Park, N. L. Nguyen, A. Ferretti, and N. Marzari, Physical Review B - Condensed Matter and Materials Physics **91**, 155112 (2015), publisher: American Physical Society.

[7] N. L. Nguyen, G. Borghi, A. Ferretti, I. Dabo, and N. Marzari, Phys. Rev. Lett. **114**, 166405 (2015).

[8] N. L. Nguyen, G. Borghi, A. Ferretti, and N. Marzari, Journal of Chemical Theory and Computation **12**, 3948 (2016), publisher: American Chemical Society.

[9] N. L. Nguyen, N. Colonna, A. Ferretti, and N. Marzari, Physical Review X **8**, 021051 (2018), publisher: American Physical Society.

[10] N. Colonna, N. L. Nguyen, A. Ferretti, and N. Marzari, Journal of Chemical Theory and Computation **14**, 2549 (2018).

[11] R. D. Gennaro, N. Colonna, E. Linscott, and N. Marzari, Bloch's theorem in orbital-density-dependent functionals: band structures from koopmans spectral functionals (2021), arXiv:2111.09550 [cond-mat.mtrl-sci].

[12] N. Colonna, N. L. Nguyen, A. Ferretti, and N. Marzari, Journal of Chemical Theory and Computation **15**, 1905 (2019), publisher: American Chemical Society.

[13] P. Hohenberg and W. Kohn, Phys. Rev. **136**, B864 (1964), publisher: American Physical Society.

[14] W. Kohn and L. J. Sham, Phys. Rev. **140**, A1133 (1965), publisher: American Physical Society.

[15] G. Onida, L. Reining, and A. Rubio, Rev. Mod. Phys. **74**, 601 (2002).

[16] L. Hedin, Phys. Rev. **139**, A796 (1965).

[17] J. McClain, Q. Sun, G. K.-L. Chan, and T. C. Berkelbach, Gaussian-based coupled-cluster theory for the ground state and band structure of solids (2017), arXiv:1701.04832 [cond-mat.mtrl-sci].

[18] W. M. C. Foulkes, L. Mitas, R. J. Needs, and G. Rajagopal, Rev. Mod. Phys. **73**, 33 (2001).

[19] J. P. Perdew, K. Burke, and M. Ernzerhof, Phys. Rev. Lett. **77**, 3865 (1996), publisher: American Physical Society.

[20] A. J. Cohen, P. Mori-Sánchez, and W. Yang, Physical Review B - Condensed Matter and Materials Physics **77**, 10.1103/PhysRevB.77.115123 (2008).

[21] J. P. Perdew, R. G. Parr, M. Levy, and J. L. Balduz, Physical Review Letters **49**, 1691 (1982), publisher: American Physical Society.

[22] J. F. Janak, Physical Review B **18**, 7165 (1978), publisher: American Physical Society.

[23] R. O. Jones and O. Gunnarsson, Rev. Mod. Phys. **61**, 689 (1989).

[24] M. Taut, Phys. Rev. A **48**, 3561 (1993).

[25] P. Giannozzi, S. Baroni, N. Bonini, M. Calandra, R. Car, C. Cavazzoni, D. Ceresoli, G. L. Chiarotti, M. Cococcioni, I. Dabo, A. Dal Corso, S. de Gironcoli, S. Fabris, G. Fratesi, R. Gebauer, U. Gerstmann, C. Gougoussis, A. Kokalj, M. Lazzeri, L. Martin-Samos, N. Marzari, F. Mauri, R. Mazzarello, S. Paolini, A. Pasquarello, L. Paulatto, C. Sbraccia, S. Scandolo, G. Sclauzero, A. P. Seitsonen, A. Smogunov, P. Umari, and R. M. Wentzcovitch, Journal of Physics: Condensed Matter **21**, 395502 (2009), publisher: IOP Publishing.

[26] P. Giannozzi, O. Andreussi, T. Brumme, O. Bunau, M. Buongiorno Nardelli, M. Calandra, R. Car, C. Cavazzoni, D. Ceresoli, M. Cococcioni, N. Colonna, I. Carnimeo, A. Dal Corso, S. de Gironcoli, P. Delugas, R. A. DiStasio, A. Ferretti, A. Floris, G. Fratesi, G. Fugallo, R. Gebauer, U. Gerstmann, F. Giustino, T. Gorni, J. Jia, M. Kawamura, H.-Y. Ko, A. Kokalj, E. Küçükbenli, M. Lazzeri, M. Marsili, N. Marzari, F. Mauri, N. L. Nguyen, H.-V. Nguyen, A. Otero-de-la Roza, L. Paulatto, S. Poncé, D. Rocca, R. Sabatini, B. Santra, M. Schlipf, A. P. Seitsonen, A. Smogunov, I. Timrov, T. Thonhauser, P. Umari, N. Vast, X. Wu, and S. Baroni, Journal of Physics: Condensed Matter **29**, 465901 (2017), publisher: IOP Publishing.

[27] J. P. Perdew and A. Zunger, Physical Review B **23**, 5048 (1981), publisher: American Physical Society.

[28] S. Kais, D. Herschbach, N. Handy, C. Murray, and G. Laming, J. Chem. Phys. **99** (1993).

[29] K.-C. Lam, F. G. Cruz, and K. Burke, International journal of quantum chemistry **69** (1998).